Cancer Cell International

RESEARCH

Open Access

Clinical relevance of macromolecular complexes involving integrins, potassium and sodium ion channels and the sodium/proton antiporter in human breast cancer

Elena Lastraioli[1,2*], Jessica Iorio[1], Francesco Piazza[2,3], Chiara Capitani[1], Michele Santillo[1,4], Claudia Duranti[1,5], Simonetta Bianchi[6], Icro Meattini[7,8], Scott P. Fraser[9], Mustafa B. A. Djamgoz[9,10], Andrea Becchetti[11] and Annarosa Arcangeli[1,2,5]

Abstract

Background Mounting evidence underline the relevance of macromolecular complexes in cancer. Integrins frequently recruit ion channels and transporters within complexes which behave as signaling hubs. A complex composed by β1 integrin, hERG1 K^+ channel, the neonatal form of the Na^+ channel Na_V 1.5 ($nNa_V1.5$) and the Na^+/H^+ antiporter NHE1 (NHE1/hERG1/β1/$nNa_V1.5$ complex) has been recently described to be expressed and regulate relevant cancer related behaviors in Breast Cancer (BCa) cells.

Methods We analyzed the expression and impact on outcome of the genes encoding the four proteins forming the NHE1/hERG1/β1/$nNa_V1.5$ complex (*SLC9A1*, *KCNH2*, *ITGB1* and *SCN5A*) in public datasets. The corresponding proteins were also evaluated by immunohistochemistry and their expression was correlated with clinic-pathological and molecular characteristics and patients' survival.

Results The expression of *KCNH2* and *SCN5A* was significantly correlated in primary BCa as occurs in the heart, although with a broader distribution, forming a functional network which also included *ITGB1* and *SLC9A1*. The co-expression proteins emerged from the immunohistochemistry analysis. Interestingly, hERG1, nNav1.5 and the hERG1/β1 integrin complex associated with several clinical features, including molecular subtype and hormone receptor status. Moreover, hERG1 and the combination of hERG1 and nNav1.5 had impact on prognosis, contributing to identifying a group of patients with worse prognosis.

Conclusions hERG1 and $nNa_V1.5$ channels along with β1 integrins and the NHE1 antiporter are co-expressed in BCa both at gene and protein levels, assembling into a macromolecular complex. The NHE1/hERG1/β1/$nNa_V1.5$ complex can be considered a novel biomarker and potential target for therapy for BCa patients.

*Correspondence:
Elena Lastraioli
elena.lastraioli@unifi.it

Full list of author information is available at the end of the article

Background

Breast cancer (BCa) is the most frequently diagnosed malignancy in the world and the leading cause of death from cancer among females [1] according to Globocan 2022 estimates (https://gco.iarc.who.int/today, accessed 25 February 26, 2024). Currently, the clinical management of BCa relies not only on the definition of "tumor, nodes and metastasis" (TNM) stage but also on the identification of the biological subtype. The disease is often sub-divided into the following: Luminal A (LA, expressing ER and/or PR and low-level Ki67), Luminal B (LB, expressing ER and/or PR and high-level Ki67), HER2-enriched (HER2, expressing high-level HER2 but not ER and PR), and triple negative (TNBC, not expressing ER, PR and HER2) [2]. The TNBC subtype is the most difficult to manage [3], thus novel biomarkers and potential therapeutic targets involved in metastasis are urgently needed.

Among emerging cancer biomarkers, ion channels represent promising candidates since they may be involved in regulating several cancer hallmarks, including metastasis [4]. Overall, functional K^+ channels, and especially voltage-gated potassium channels (K_Vs), are frequently de-regulated in cancer [5]. These include hERG1 (also named K_V11.1, encoded by *KCNH2* gene) which is over-expressed and functional dysregulated in a wide range of human cancer cells and tissues and associate clinical outcome [6, 7]. Interestingly, hERG1 was shown to be expressed in BCa primary tissues belonging to all the different molecular subtypes and its expression contributes to favorable patient outcome [7].Voltage-gated sodium channels (Na_Vs) are also expressed in several carcinomas [8]. In BCa, upregulation of Na_V expression promotes invasiveness and metastasis [9–11]. The predominant functional Na_V subtype is Na_V1.5 (encoded by *SCN5A* gene) [10–12]. Nav1.5 promotes BCa invasiveness by promoting H^+ efflux via Na^+/H^+ exchange [13]. Particularly intriguing is the demonstration that this channel is expressed in its neonatal splice form (nNa_V1.5) [11], resulting from the alternative splicing of exon 6 with the "adult" and "neonatal" forms differing in the S3-S4 region of domain I by several amino acids [10]. nNa_V1.5 is an 'oncofetal' channel not expressed in healthy adult tissues [14].

Ion channels are frequently present on the cell plasma membrane as macromolecular complexes with functionally interactive components [15]. In particular, hERG1 physically associates with β1 integrin (encoded by the *ITGB1* gene), and the complex enhances the metastatic potential of BCa in vivo [16]. Conversely, when the association is reduced, metastatic tendency is inhibited [16]. In colorectal cancer, the hERG1/β1 integrin complex activates PI3K signaling and promotes migration, invasion and autophagy [17]. Moreover, Kv and Nav channels are well known to function interactively, as they do in the most basic of electrophysiological activities, the action potential [17].

We recently described a novel plasma membrane macromolecular complex formed by hERG1, the neonatal form of Na_V1.5, the β1 subunit of integrin receptors and the Na^+/H^+ antiporter NHE1 in BCa cells, in particular Triple Negative BCa (TNBC). Due to the orientation and linking between the different proteins, the complex was addressed as NHE1/hERG1/β1/nNa_V1.5. Complex formation is triggered by integrin activation (e.g. by cell adhesion onto Fibronectin) and controls BCa cell migration and invasiveness). Within the complex the two channels are mutually regulated, hence blocking one or the other produces the same functional effects, which are due to the disassembly of the complex. The activation of the complex causes the cytoplasmic alkalinization mediated by NHE1 leading to the modulation of f-actin organization and thus to the regulation of cell migration and invasiveness [18].

Moving down this line, the present paper aimed to determine (i) the presence of the above macromolecular complex formed by NHE1, β1 integrins, hERG1 and nNav1.5 in human BCa tissues, and (ii) the clinical relevance of the components of the complex on patients' survival.

Results

The genes encoding the four components of the NHE1/hERG1/β1/nNa_V1.5 complex (*SLC9A1*, *KCNH2*, *ITGB1* and *SCN5A*) are expressed in human BCa primary samples and correlate with clinical outcome: in silico analysis

To define whether the NHE1/hERG1/β1/nNa_V1.5/complex identified in BCa cells [18] could have translational relevance to BCa patients, we first performed an in-silico analysis to evaluate the expression of the corresponding genes *SLC9A1*, *KCNH2*, *ITGB1* and *SCN5A* in BCa primary samples ($n = 1099$) compared to healthy breast tissue ($n = 179$). Data were retrieved from TGCA and GTEx datasets and analyzed through UCSC Xena Browser tools (details in the Materials and Methods section and in the legend to Fig. 1). The volcano plot of differentially expressed genes (DEGs) in TCGA invasive breast adenocarcinoma samples (Fig. 1A) shows that many genes are either down-regulated (blue dots, $N = 3417$) or up-regulated (red dots, $N = 2398$) while a smaller proportion of genes appears not to be differentially expressed (grey dots). Some DEGs known to be associated with BCa are labeled in the plot. Moreover, Gene Set Variation Analysis (GSVA) clearly indicated a broader distribution of DEGs in BCa compared to healthy tissue samples ($P < 0.0001$, Fig. 1B). Additionally, we evaluated whether GSVA differed across the molecular subtypes of BCa (Fig. 1C) and TNM stages (Fig. 1D). In these cases,

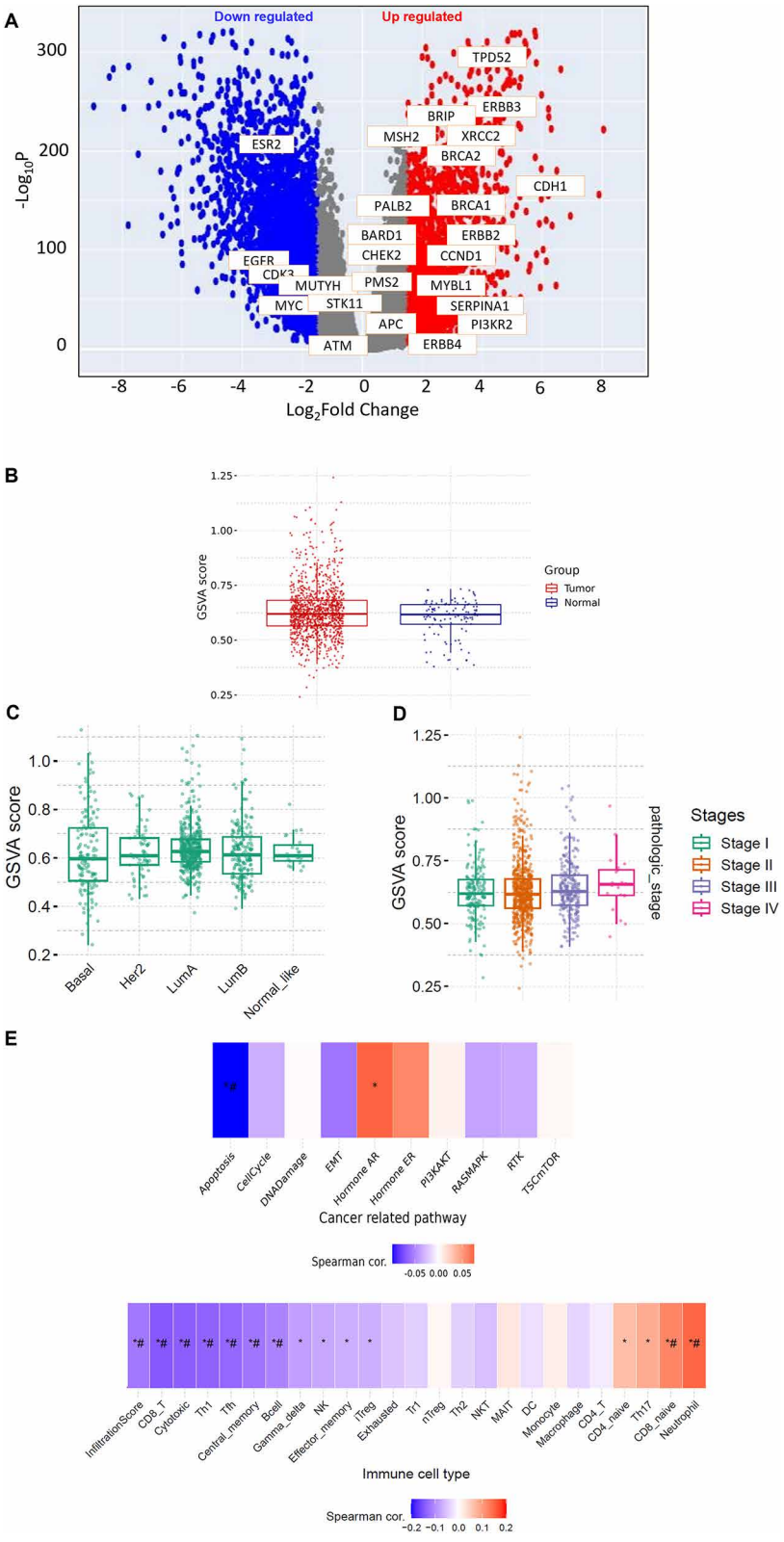

Fig. 1 (See legend on next page.)

(See figure on previous page.)

Fig. 1 In-silico analyses of breast cancer datasets. **A**) Volcano plot showing DEGs between healthy breast and BCa. The plot was drawn using UCSC Xena Browser (http://xena.ucsc.edu/). **B**) Box plot comparing the GSVA score in BCa (red) and healthy breast (blue). Log2 fold change (Tumor/Healthy): 0.08, $P < 0.0001$. The analysis was carried out with the Gene Set Cancer Analysis (GSCA) tools (https://guolab.wchscu.cn/GSCA). **C**) GSVA score in the different molecular subtypes ($P = 0.130$). **D**) GSVA score in the four TNM stages ($P = 0.310$). **E**) Correlation between GSVA and cancer-related pathways (left graph, *P value ≤ 0.05; #: FDR ≤ 0.05; Apoptosis: FDR = 0.033, $P = 0.003$; Cell cycle: FDR = 1, $P = 0.3145$; DNA damage: FDR = 1, $P = 0.9616$; EMT: FDR = 0.6062, $P = 0.0792$; Hormone AR: FDR = 0.2269, $P = 0.0252$; Hormone ER: FDR = 0.6062, $P = 0.0758$; PI3KAKT: FDR = 1, $P = 0.2449$; RTK: FDR = 1, $P = 0.2768$; TSCmTOR: FDR = 1, $P = 0.9166$) and Immune cell types (right graph, *P value ≤ 0.05; #: FDR ≤ 0.05; CD4 naïve: FDR = 0.2775, $P = 0.0230$; CD8 naïve: FDR = 0.0008, $P < 0.0001$; Cytotoxic: FDR < 0.0001, $P < 0.0001$; Exhausted: FDR = 0.8367, $P = 0.0930$; Tr1: FDR = 1, $P = 0.1670$; nTreg: FDR = 1, $P = 0.7711$; iTreg: FDR = 0.2775, $P = 0.0239$; Th1: FDR = 0.0001, $P < 0.0001$; Th2: FDR = 1, $P = 0.1775$; Th17: FDR = 0.0625, $P = 0.0039$; Tfh: FDR = 0.0002, $P < 0.0001$; Central Memory: FDR = 0.0013, $P < 0.0001$; Effector Memory: FDR = 0.2775, $P = 0.0213$; NKT: FDR = 0.6675, $P = 0.0667$; MAIT: FDR = 1, $P = 0.3933$; DC: FDR = 1, $P = 0.3696$; B cell: FDR = 0.0057, $P = 0.0003$; Monocyte: FDR = 1, $P = 0.5549$; Macrophage: FDR = 1, $P = 0.2284$; NK: FDR = 0.1693, $P = 0.0121$; Neutrophil: FDR < 0.0001, $P < 0.0001$; Gamma delta: FDR = 0.0894, $P = 0.0059$; CD4 T: FDR = 1, $P = 0.5701$; CD8 T: FDR < 0.0001, $P < 0.0001$; Infiltration score: FDR: 0.0016, $P < 0.0001$). The analysis was carried out with the Gene Set Cancer Analysis (GSCA) tools (https://guolab.wchscu.cn/GSCA)

although the distribution was wider in certain molecular subtypes (such as for example Basal-like and Luminal A/B) compared to others (e.g. Normal-like BCa) no statistically significant association were observed ($P = 0.130$ and $P = 0.310$, respectively). Finally, GSVA was applied to investigate well-established pathways in cancer biology and immune system involvement (Fig. 1E), revealing varying associations between GSVA scores and cancer characteristics. For example, as indicated by Spearman correlation coefficients, hormone receptors were positively associated (red bars) whilst apoptosis had a negative association (blue bar). Similarly, the association was negative with infiltration, CD8, Th1 and Th2 among others (blue bars, Fig. 1E), while there was a positive association with neutrophils and CD4 and CD8 naïve cells (red bars, Fig. 1E).

Next, a detailed bioinformatic analysis was carried out to unravel the profile of DEGs in samples of BCa compared with healthy breast tissue. This revealed that several GO terms and KEGG pathways turned out to be significantly upregulated in BCa (Fig. 2A and B, respectively). Among them, particularly relevant are GO terms related to microtubules and KEGG pathways associated with cell cycle, tight junctions and DNA replication (as highlighted by the FDR and P values reported in the tables on the right). On the other hand, none of the downregulated terms and pathways appear to be statistically significantly associated with BCa, possibly because they are general terms not directly related to this malignancy.

Moreover, from analysis of the Molecular Signatures Database (MSigDB) hallmark gene set collection for BCa proposed by Liberzon and colleagues [20], it can be seen that several genes (such as Estrogen Response, G2M checkpoint, mitotic spindle, among others) are upregulated (indicated in red in Figure S1).

The analysis of the above-mentioned genes (*SLC9A1*, *KCNH2*, *ITGB1* and *SCN5A*) showed variable levels of expression of the four transcripts, with very infrequent somatic mutations and copy number variations (Fig. 3).

Furthermore, we studied whether *SLC9A1*, *KCNH2*, *ITGB1* and *SCN5A* were differentially expressed in BCa with respect to healthy breast tissue and we analyzed the same TCGA cohort as above. In Fig. 4A, we report the expression of the four genes of interest in healthy breast (blue dots and curves), human heart (orange dots and curves) and BCa (green dots and curves). Interestingly, the four genes were found to be deregulated in these tumor samples with respect to healthy breast. The distribution of the expression levels of *KCNH2*, *SCN5A* and *SLC9A1* appear to display a marked dependency on the specific tissue within the BCa cohort (see the first, second and fourth rows of Fig. 4A). In contrast, *ITGB1* displays a clearly stable distribution pattern that does not depend on the specific tissue (see third row in Fig. 4A). More specifically, there seems to be an overall trend toward broader distributions of expression levels of *KCNH2*, *SCN5A* and *SLC9A1* in tumor samples (see curves in the diagonal panels on Fig. 4A). Interestingly, this tendency is the most evident for *KCNH2*, which unquestionably shows a more restricted amplitude of expression in healthy breast with respect to the tumor sample (see the blue distribution in Fig. 4A, first row).

As expected, the expression levels of *KCNH2* and *SCN5A* in the human heart orange dots in Fig. 4A) are high and display a high degree of correlation. This feature is specifically highlighted by the contour plots in Fig. 4B (which provides a different representation of panel (2,1) in Fig. 4A). The heart is considered a reference, as it is known that *SCN5A* and *KCNH2* expression levels are tightly correlated in this tissue, and the two channels play a major role in cardiac function [21, 22]. The evaluation of the four genes in other healthy tissues (muscle, brain, thyroid, colon, lung, adipose tissue, nerve, small intestine, esophagus, skin, liver) was also performed but the heart proved to be the tissue with the highest expression levels of the two channels, as expected (Figures S2-S5) As expected, *ITGB1* gene and the corresponding protein are widely expressed in heathy tissues, generally displaying high levels of expression (Figure S6). Besides confirming that the two channels are highly expressed in this tissue, a clear correlation is evident, highlighted by the elongated shape of the contour lines. In contrast, when analyzing healthy breast and BCa samples, it emerged clearly that

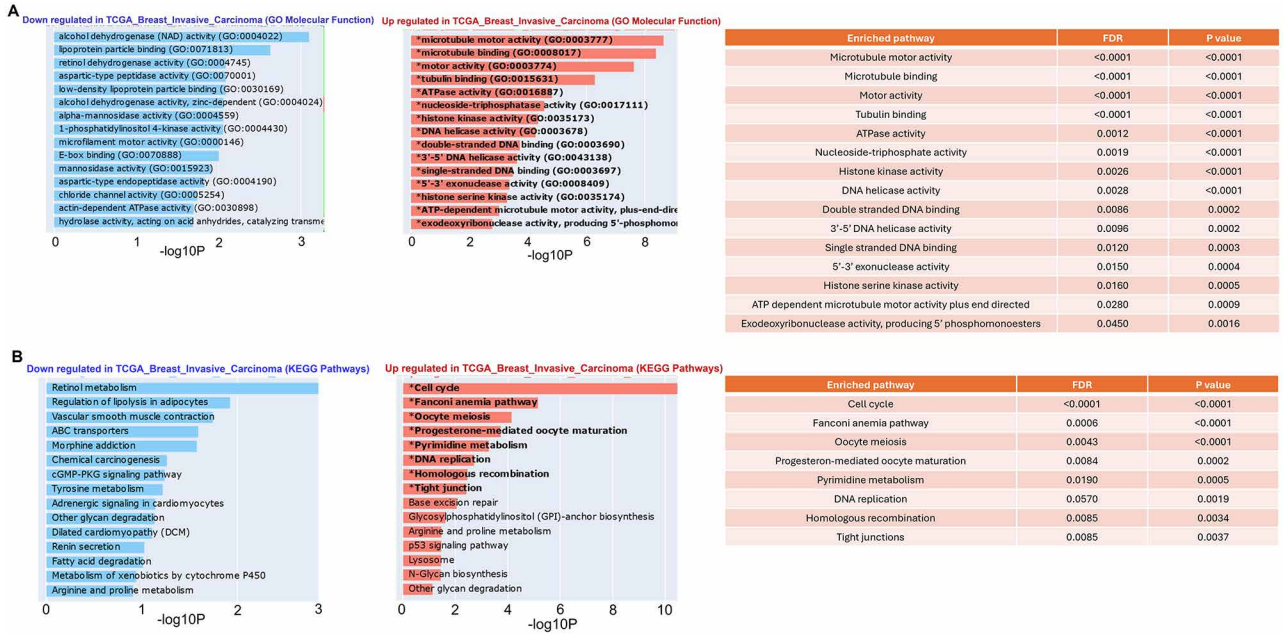

Enriched pathway	FDR	P value
Microtubule motor activity	<0.0001	<0.0001
Microtubule binding	<0.0001	<0.0001
Motor activity	<0.0001	<0.0001
Tubulin binding	<0.0001	<0.0001
ATPase activity	0.0012	<0.0001
Nucleoside-triphosphate activity	0.0019	<0.0001
Histone kinase activity	0.0026	<0.0001
DNA helicase activity	0.0028	<0.0001
Double stranded DNA binding	0.0086	0.0002
3'-5' DNA helicase activity	0.0096	0.0002
Single stranded DNA binding	0.0120	0.0003
5'-3' exonuclease activity	0.0150	0.0004
Histone serine kinase activity	0.0160	0.0005
ATP dependent microtubule motor activity plus end directed	0.0280	0.0009
Exodeoxyribonuclease activity, producing 5' phosphomonoesters	0.0450	0.0016

Enriched pathway	FDR	P value
Cell cycle	<0.0001	<0.0001
Fanconi anemia pathway	0.0006	<0.0001
Oocyte meiosis	0.0043	<0.0001
Progesteron-mediated oocyte maturation	0.0084	0.0002
Pyrimidine metabolism	0.0190	0.0005
DNA replication	0.0570	0.0019
Homologous recombination	0.0085	0.0034
Tight junctions	0.0085	0.0037

Fig. 2 In-silico enrichment analyses of breast cancer datasets. **A**) GO enrichment analysis relative to Molecular Function carried out in TCGA/GTex databases. The table on the right shows the FDR and P values of the significantly enriched GO terms. The analysis was performed through the Enrichr web tool [19]. **B**) KEGG pathway analysis showing downregulated (in blue) and upregulated (in red) pathways in BCa compared to healthy breast tissue. Significant terms are highlighted in bold. The table on the right shows the FDR and P values of the significant pathways. The analysis was performed through the Enrichr web tool

the expression levels of the two genes are uncorrelated, as highlighted by the much more circular shapes of the contour lines (blue and green curves in Fig. 4B). However, it also emerged that the range of variability of both expression levels nearly doubles in BCa samples with respect to healthy tissues. In particular, the highest expression levels of *KCNH2* are seen to overlap with the low-expression region found in the human heart, while in healthy breast tissues *KCNH2* expression levels are well separated from those in the heart.

To examine the degree of correlation more closely between *KCNH2* and *SCN5A*, a correlation analysis was carried out by isolating patient subgroups for which the expression levels $\boldsymbol{E}_k$ ($k = KCNH2$, $SCN5A$) among the overall populations of N_k samples were larger than the respective median plus a variable fraction q of the respective standard deviation s_k. More precisely, for a given value of q, we selected those patients i ($i = 1,2, \ldots, N_k$) for which $E_k(i) > \mathrm{med}(E_k) + qs_k$, (and then isolating two equal-number populations corresponding to the intersection of the two selected subgroups). We chose to limit the subdivision so that subgroups contained a minimum of 30 samples each. The purpose of this analysis is to better discriminate whether a correlation might be present only in a definite range of (high) expression. The analysis was performed on the entire TCGA cohort, without subdividing the patients according to molecular subtype. As reported in Fig. 4C, *KCNH2* and *SCN5A* indeed showed a consistent trend, where a positive, increasing correlation is seen to emerge as the subgroups include higher and higher levels of expression, reaching a quasi-steady value of 0.3 in the interval $\mathrm{med}(E_k) + s_k < E_k < \mathrm{med}(E_k) + 1.5\, s_k$, only in BCa. By contrast, in healthy breast no correlation was seen to emerge in subgroups of patients at higher levels of expression (blue curves). This conclusion is also confirmed by splitting *KCNH2* and *SCN5A* expression according to the median values (Fig. 4D and E, respectively).

Overall, the analyses presented here strongly hint for the first time at a correlation among high expression levels of *KCNH2* and *SCN5A* genes in BCa, suggesting that the two channels might cooperate in these cells when their expression levels fall within a specific range on the high-expression side.

We then performed a network analysis to evaluate whether the association between NHE1, hERG1, β1 integrin and nNav1.5 found in BCa cells [18] was also present at gene level in primary samples. Figure 5A shows that the four genes (indicated by the red stars) are 'connected' with the involvement of several other coding genes (indicated by the blue circles) and a pseudogene (indicated by the lilac circle). The list of genes involved in the network is reported in Table 1.

Finally, we performed a survival analysis, first considering the four genes of interest separately and then in combinations. Data were retrieved from TCGA and the

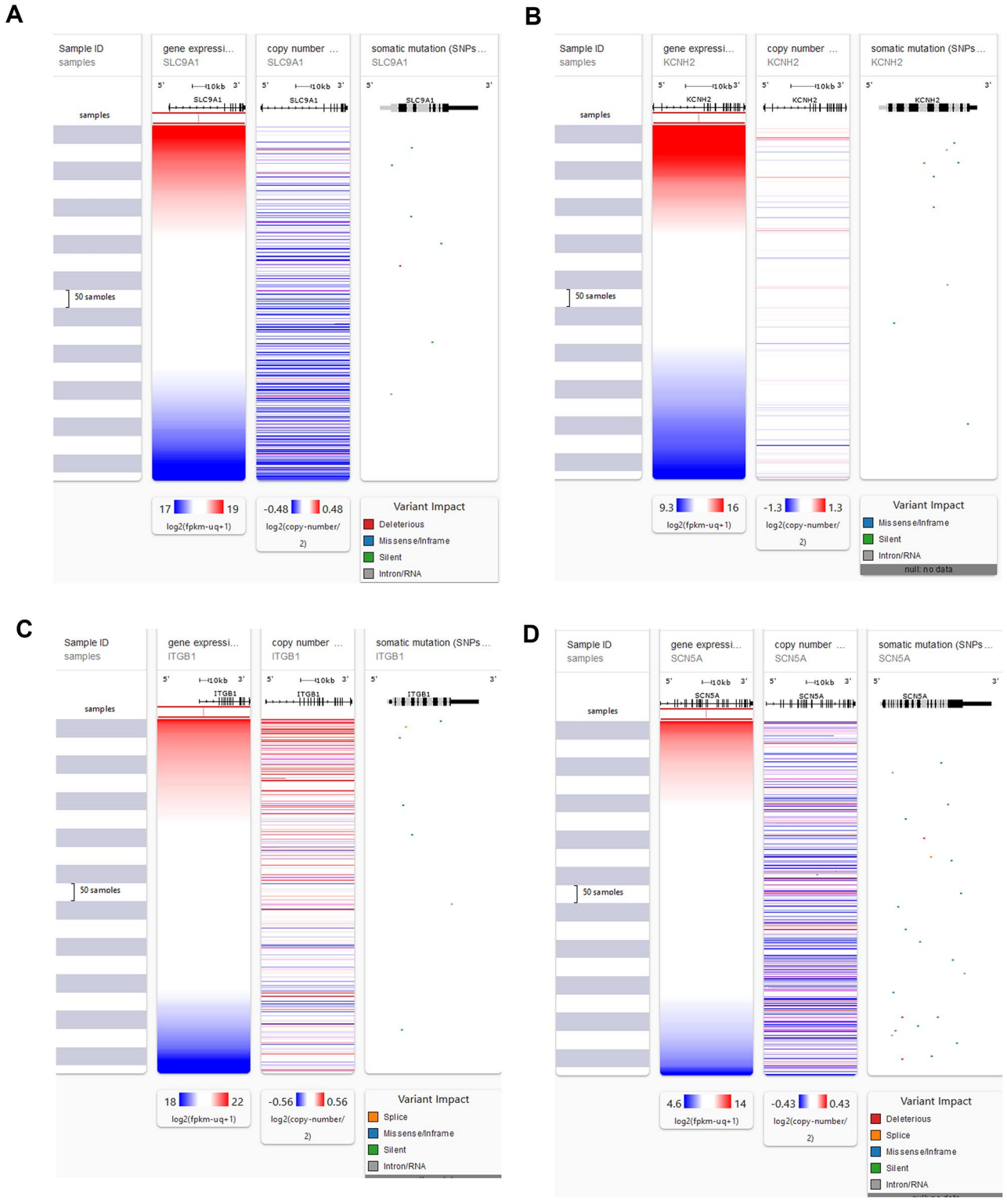

Fig. 3 Gene expression and somatic mutations for *SLC9A1* (**A**), *KCNH2* (**B**), *ITGB1* (**C**) *and SCN5A* (**D**) on a cohort of 1284 BCa from TCGA database. The analysis was carried out through UCSC Xena Browser

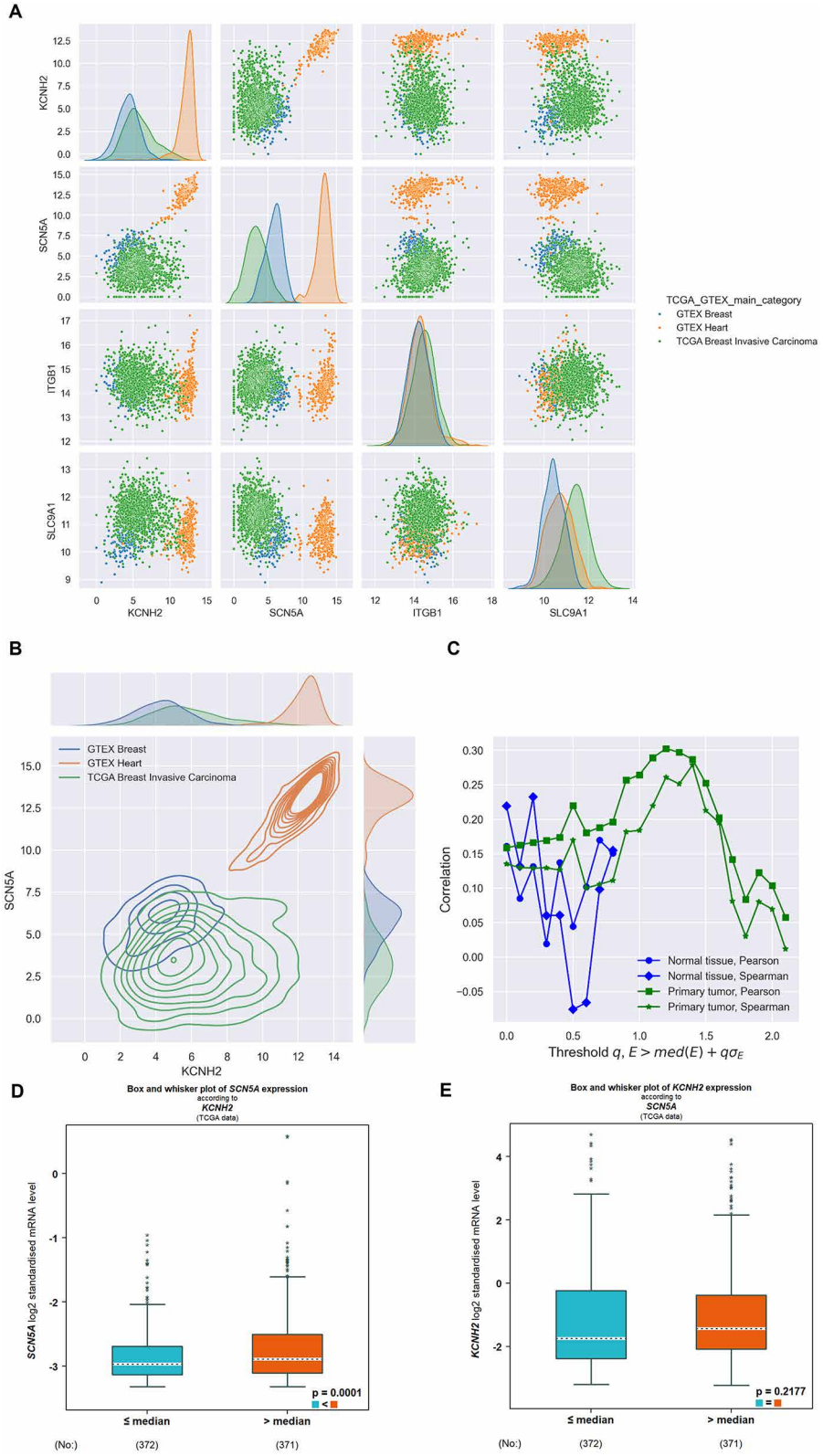

Fig. 4 (See legend on next page.)

(See figure on previous page.)

Fig. 4 In-silico analyses of *KCNH2*, *SCN5A*, *ITGB1* and *SLC9A1* in BCa samples. **A**) Joint expression correlation plots for *KCNH2*, *SCN5A*, *ITGB1* and *SLC9A1* in BCa (green dots and curves), healthy breast (blue dots and curves) and human heart (orange dots and curves). The curves on the diagonal panels represent plots of kernel density distributions of expression. **B**) Contour plot showing *KCNH2* and *SCN5A* expression in BCa (orange curves) and healthy breast (blue curves). Human heart (orange curves) is also reported as a reference since it is well known that in this tissue both channels are highly expressed and functionally associated. **C**) Variable-subgroup correlation analysis (see text for details) between *KCNH2* and *SCN5A* in healthy breast (blue curves) and BCa (green curves). In healthy breast no correlation is evident, while in BCa patients the expression of the two genes follows a similar trend, displaying a consistently increasing correlation in higher and higher-expression subgroups, reaching a maximum quasi-steady correlation value of 0.3 in a relatively wide region of expression. An almost identical result is observed using both Pearson and Spearman correlation tests. Data are reported as fpkm-uq. **D**) Correlation analysis of *KCNH2* and *SCN5A* in BCa datasets from TCGA according to *KCNH2* expression levels. The threshold was set at the median value. **E)** Correlation analysis of *KCNH2* and *SCN5A* in BCa datasets from TCGA according to *SCN5A* expression levels. The threshold was set at the median value. The analyses were performed with Breast Cancer Gene-Expression Miner v5.0 (bc-GenExMiner v5.0)

number and frequency for each subgroup are reported in Table 2.

Patients with higher levels of *ITGB1* and *SCN5A* (blue curves in Fig. 5D and E, respectively) had shorter Overall Survival (OS) and these were statistically significant ($P = 0.0033$ and $P = 0.0005$, respectively); the OS of patients was shorter for middle levels of *KCNH2* although significance was not reached (orange curve in the Kaplan Meier plot in Fig. 5C). For *SLC9A1*, there was no difference (Fig. 5B). When considering only two groups (low and high expression) no trend could be observed for any marker (not shown).

Combined KM analysis showed that there was a tendency for patients expressing low levels of *KCNH2* and high *SCN5A* (panel A), *ITGB1* (panel B) and *SLC9A1* (panel C) to have shorter OS, although significance was not reached (Figure S7). The other combined KM plots were not impressive (Figure S8).

NHE1, hERG1, β1 integrins and nNa$_v$1.5 proteins are co-expressed in human BCa primary samples

The above four proteins were then studied in human BCa samples applying the IHC technique. In particular, we determined the specific expression of the neonatal form of the Na$_V$1.5 (whose transcript is not stored as a separate entity in public datasets) using the novel nNav1.5-specific mAb which was developed by us (Duranti C et al., manuscript in preparation). Furthermore, we also evaluated the quantitative expression of either the hERG1 protein (using the hERG1 mAb) or of the hERG1/β1 integrin complex (using a bispecific antibody targeting the two proteins (scDb-hERG1-β1) [24, 25] (in the Materials and Methods section all the details about the antibody and protocols used are reported). The expression of the β1 integrin alone was not determined, but only the expression of the adhesion receptor bound to hERG1 through the scDb-hERG1-β1 which has already given good results in different cancers. We performed a retrospective study on 81 cases of primary BCa encompassing the four main molecular subtypes [7]. The clinical features of the cohort are reported (Table 3).

It emerged that while neither of the protein is expressed in normal breast tissue (Fig. 6A), the four proteins are expressed in tumor samples (Fig. 6B-E), although in a different percentage of cells and at a different intensity. Interestingly, the four proteins were co-expressed in the same tumor sample and in the same cells (see the representative pictures in Fig. 6F, where positive cells are indicated by the brown color). The concomitant expression of the proteins was further confirmed quantitatively by the Spearman Correlation Coefficient (see the heatmap in Fig. 6G).

We then analyzed the associations between the IHC scoring of the proteins of interest and clinico-pathological features. Several statistically significant associations emerged when considering the scoring categories as defined in Materials and Methods (Table 4). In particular, hERG1 as well as the hERG1/β1 integrin complex were associated with molecular subtype, being highly expressed (score 3) in Luminal A samples. High level of nNa$_v$1.5 expression was associated with Luminal B subgroup. Middle expression (Score 2) of hERG1 and the hERG1/β1 integrin complex was also associated with G2 tumors. Interestingly, the expression of the two channels as well as of the hERG1/β1 integrin complex was significantly positively associated with the expression of hormone receptors (ER and PgR). Both hERG1 and the hERG1/β1 integrin complex were associated with HER2 expression. No statistically significant association emerged between NHE1 scoring and clinico-pathological features.

hERG1, hERG1/β1 and nNa$_v$1.5 have an impact on BCa patients' survival

We then performed a survival analysis subdividing the samples according to their scoring. As shown in Fig. 7, hERG1 score 2 (middle expression) was associated with shorter OS (orange curve in Fig. 7A; $P = 0.0005$). The same trend was observed for PFS and DMFS (panels B and D) although significance was not reached. On the whole, these finding agree with the data derived from the TCGA dataset analysis. Equivalent analyses were carried out for hERG1/β1 integrin complex (Fig. 7E-H). The same trends in PFS, LRFS and DMFS observed for hERG1 were also detected evaluating the expression of the complex, with a statistically significant value for LRFS ($P = 0.0390$).

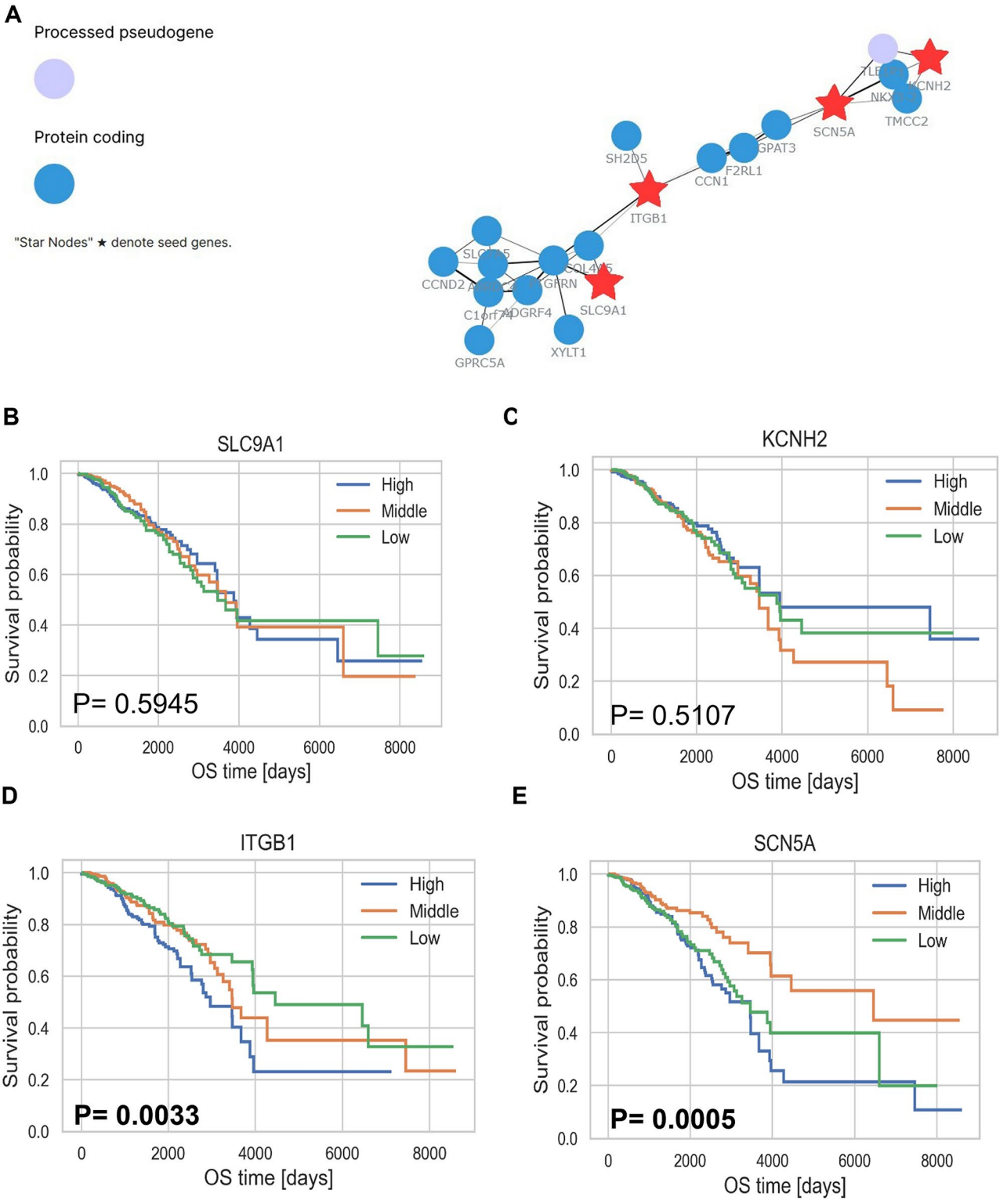

Fig. 5 In-silico network and survival analyses of *SLC9A1*, *KCNH2*, *ITGB1* and *SCN5A* in BCa samples. **A**) Network analysis of *SLC9A1*, *KCNH2*, *ITGB1* and *SCN5A*, and in BCa datasets. The genes of interest (seed genes) are indicated by red stars while circles represent the correlated genes. Pearson Correlation Threshold:0.46; Top genes: 15. The analysis was performed with GeneFriends [23]. **B-E**) Survival analysis of in-silico BCa cohort ($N = 1203$). Kaplan Meier plots of OS for *SLC9A1* (panel **B**), *KCNH2* (panel **C**), *ITGB1* (panel **D**) and *SCN5A* (panel **E**). Blue curves: high expression; Orange curves: middle expression; Green curves: low expression. The in-silico analyses were carried out through in a TCGA BCa dataset retrieved by UCSC Xena Browser

Table 1 Top 15 co-expressed genes within *KCNH2*, *SCN5A*, *ITGB1* and *SLC9A1* gene network. The analysis was performed with GeneFriends (https://www.genefriends.org/) [23]

Gene name	Description
NKX3-2	NK3 Homeobox 2
TMCC2	Transmembrane And Coiled-Coil Domain Family 2
GPAT3	Glycerol-3-Phosphate Acyltransferase 3
F2RL1	F2R Like Trypsin Receptor 1
CCN1	Cellular Communication Network Factor 1
SH2D5	SH2 Domain Containing 5
COL4A5	Collagen Type IV Alpha 5 Chain
PTGFRN	Prostaglandin F2 Receptor Inhibitor
SLC7A5	Solute Carrier Family 7 Member 5
ARRDC4	Arrestin Domain Containing 4
CCND2	Cyclin D2
C1orf74	Chromosome 1 Open Reading Frame 74
ADGRF4	Adhesion G Protein-Coupled Receptor F4
GPRC5A	G Protein-Coupled Receptor Class C Group 5 Member A
XYLT1	Xylosyltransferase 1

Table 2 Number of samples and frequency for *KCNH2*, *SCN5A*, *ITGB1* and *SLC9A1* subgroups of expression

		N	Frequency
KCNH2 (N = 1203)	**Low expression**	400	33.25%
	Middle expression	402	33.42%
	High expression	401	33.33%
SCN5A (N = 1203)	**Low expression**	397	33.00%
	Middle expression	403	33.50%
	High expression	403	33.50%
ITGB1 (N = 1203)	**Low expression**	399	33.17%
	Middle expression	402	33.42%
	High expression	402	33.42%
SLC9A1 (N = 1203)	**Low expression**	402	33.42%
	Middle expression	404	33.58%
	High expression	397	33.00%

Table 3 Clinical and molecular features of the patients enrolled in the study

		N	Frequency
Molecular Subtype	***Luminal A***	23	28.40%
	Luminal B	20	24.69%
	HER2+	20	24.69
	Triple Negative	18	22.22
Grading	***G1***	14	17.50%
	G2	16	20.00%
	G3	50	62.50%
TNM stage	***I***	52	64.20%
	II	18	22.22%
	III	10	12.35%
	IV	1	1.23%
Metastases	***No***	71	87.65%
	Yes	10	12.35%
Relapse	***No***	76	93.83%
	Yes	5	6.17%
ER	***Negative***	36	44.44%
	Positive	45	55.56%
PgR	***Negative***	40	49.38%
	Positive	41	50.62%
HER2	***Negative***	28	34.57%
	Score 1	9	11.11%
	Score 2	15	18.52%
	Score 3	**29**	35.80
Ki67	***≤ 20%***	20	24.69
	> 20%	61	75.31

The survival analyses performed taking into account $nNa_V1.5$ and NHE1 expression levels did not highlight any statistically significant association or trend (Figures S7 and S8).

As previously carried out for TCGA data, combined Kaplan Meier curves were built for all the proteins analyzed. The combination between hERG1 and $nNa_V1.5$ had an impact on OS, with samples with middle hERG1 expression and high nNav1.5 expression having a shorter survival ($P = 0.0030$, orange curve in Fig. 8). No statistically significant association emerged for the other combinations, in accordance with what reported for the corresponding genes (Figures S9-S13).

Discussion

BCa still represents a big challenge for clinicians and a relevant medical need for the scientific and medical community due to the high incidence of the disease, to the occurrence of hard-to-treat tumors (i.e. Triple Negative molecular subtype) and to the development of resistance to treatment. For these reasons scientific research has been pushed in the last years in order to better define the molecular pattern of BCa and hopefully to identify novel potential biomarkers for the management of the patients. In the last twenty years the role of ion channels and transporters and of the macromolecular complexes they form have been investigated in several tumors also comprising BCa. Previously, we shown that hERG1 (potassium channel encoded by the *KCNH2* gene) are expressed in primary BCa and characterize patients with longer progression-free survival, local relapse free-survival and metastases-free survival [7]. More recently, we further contributed to the field of BCa studies identifying a β1 integrin centered macromolecular complex comprising hERG1, nNav1.5 (the neonatal isoform of the sodium channel encoded by *SCN5A*) and NHE1 (the Na^+/H^+ antiporter encoded by the *SLC9A1* gene) in BCa cells [18].

In the present paper, we moved forward, and we showed that not only hERG1 channel alone but also the macromolecular complex is expressed in primary BCa. This conclusion derives from both an in-silico analysis on BCa primary samples, and by an IHC study performed on a cohort of 81 BCa samples of different molecular subtypes. Moreover, we highlighted several associations with

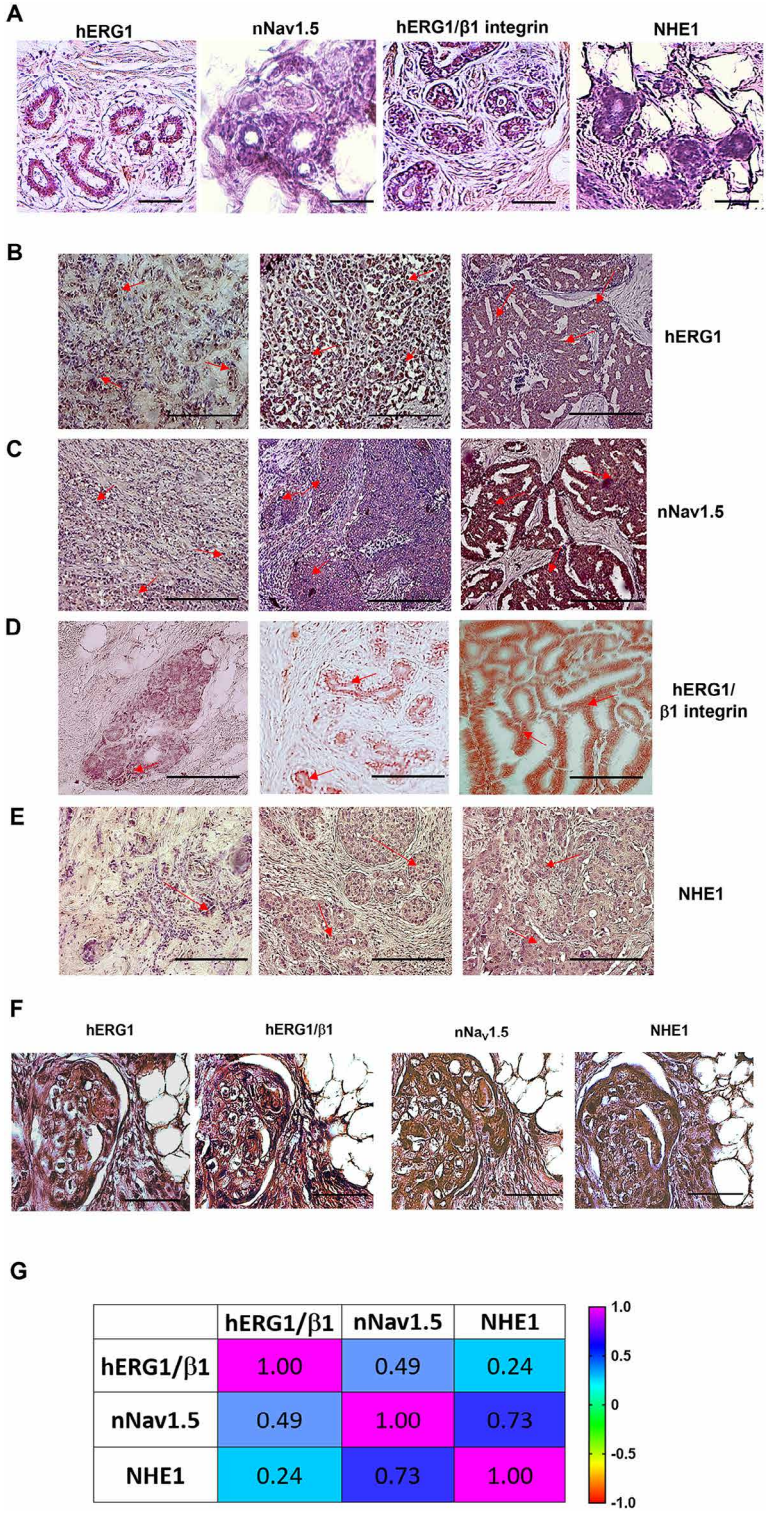

Fig. 6 Immunohistochemical evaluation of the expression of hERG1, hERG1/β1, $nNa_V1.5$ and NHE1 in human primary BCa. IHC experiments and assessment of score were performed as reported in the Materials and Methods section. Representative sections of healthy breast for each marker (**A**). Original magnification ×200. Scale bar: 100 µm. Representative examples of Score 1, Score 2 and Score 3 are reported for hERG1 (**B**), nNav1.5 (**C**), hERG1/β1 integrin complex (**D**) and NHE1 (**E**). Original magnification ×200. Scale bar: 100 µm. (**F**) Concomitant expression of hERG1, hERG1/β1 integrin complex, nNav1.5 and NHE1 in the same cells of a representative sample. Original magnification ×400. Scale bar: 50 µm. (**G**) Heatmap showing the Spearman Correlation Coefficient for hERG1/β1 integrin complex, nNav1.5 and NHE1. All the P values are statistically significant ($P < 0.0001$)

Table 4 Association between hERG1, nNav1.5, hERG1/β1 and NHE1 expression and clinicopathological/molecular features. *: $p<0.05$ (Fisher exact test)

Clinical/molecular feature (number of patients)		hERG1 *P* value	hERG1/β1 *P* value	nNav1.5 *P* value	NHE1 *P* value
Molecular Subtype	*Luminal A (23)* *Luminal B (20)* *HER2+(20)* *Basal-like (18)*	**0.016*** (Score 3 and Luminal A)	**0.005*** (Score 3 and Luminal A)	**0.047*** (Score 3 and Luminal B)	0.638
Grading	*G1(9)* *G2 (25)* *G3 (41)*	**0.023*** (Score 2 and G2)	**0.026*** (Score 2 and G2)	0.052	0.086
TNM stage	*I (52)* *II (18)* *III (10)* *IV (1)*	0.112	0.609	0.780	0.053
Metastases	*No (71)* *Yes (10)*	0.477	0.822	0.152	0.461
Relapse	*No (76)* *Yes (5)*	0.427	0.353	0.214	0.538
ER	*Negative (36)* *Positive (45)*	**0.001*** (Score 3 and ER positive)	**0.001*** (Score 3 and ER positive)	**0.002*** (Score 2 and ER positive)	0.223
PgR	*Negative (40)* *Positive (41)*	**0.005*** (Score 3 and PgR positive)	**0.001*** (Score 3 and PgR positive)	**< 0.001*** (Score 3 and PgR positive)	0.192
HER2	*Negative (28)* *Score 1 (9)* *Score 2 (15)* *Score 3 (29)*	**0.020*** (Score 2 and HER2 Score 1)	**0.009*** (Score 3 and HER2 Score 1)	0.141	0.599
Ki67	*≤ 20% (23)* *> 20% (58)*	0.131	0.078	0.250	0.061

clinical features and outcome. Finally, we showed that in primary samples the pattern of the combined expression of the two ion channels involved in the macromolecular complex (hERG1 and nNav1.5) significantly correlates with survival.

SLC9A1, *KCNH2*, *ITGB1* and *SCN5A* genes in BCa

Through an in-silico approach we investigated the gene expression profile of BCa and we found that, among the high number of DEGs also *SLC9A1*, *KCNH2*, *ITGB1* (encoding the β1 integrin) and *SCN5A* displayed variable expression levels, with very rare somatic mutations and copy number variations. To the best of our knowledge only the paper by Fukushiro-Lopes and colleagues [26] evaluated the expression of *KCNH2* gene in BCa: analyzing Oncomine dataset the Authors showed that the expression of the gene was higher in BCa with respect to healthy breast but did not go deeper in the analysis. Therefore, our paper provides the first genetic characterization of *KCNH2* in BCa performed in a wide cohort of patients whose data are stored in TCGA databases. From such analysis we showed that patients expressing middle levels of *KCNH2* are characterized by lower overall survival. The expression and relevance of *ITGB1* gene in BCa was investigated by other groups and it was highlighted that high levels of expression were associated with lower distant metastases free survival [27]. Moreover, from a metanalysis aimed at elucidating the role of *ITGB1* in human cancers it was shown that high levels of expression were associated with poorer outcome (shorter Overall and Disease-free survival) [28]. These results are in accordance with the data reported in this paper, obtained through the analysis of a large TCGA cohort in fact we highlighted a statistically significant association between high *ITGB1* levels of expression and shorter OS. For *SLC9A1*, the expression of the gene was found to be higher in BCa than in healthy breast [29] but studies evaluating associations with clinical features and outcome are lacking. Therefore, our paper is the first one reporting that the levels of expression of the gene have no effect on overall survival. Finally, the expression of *SCN5A* has been evaluated by Yang and colleagues in the Oncomine dataset and it was shown that the gene has a higher level of expression in BCa with respect to healthy breast tissue and that high *SCN5A* levels were associated with poor prognosis [30] in accordance with the data presented in this paper. The in-silico analysis indicates that the *SLC9A1* and *KCNH2* genes, as single entities, are not associated with survival. This finding strengthens our hypothesis that the main relevance lies in the complex

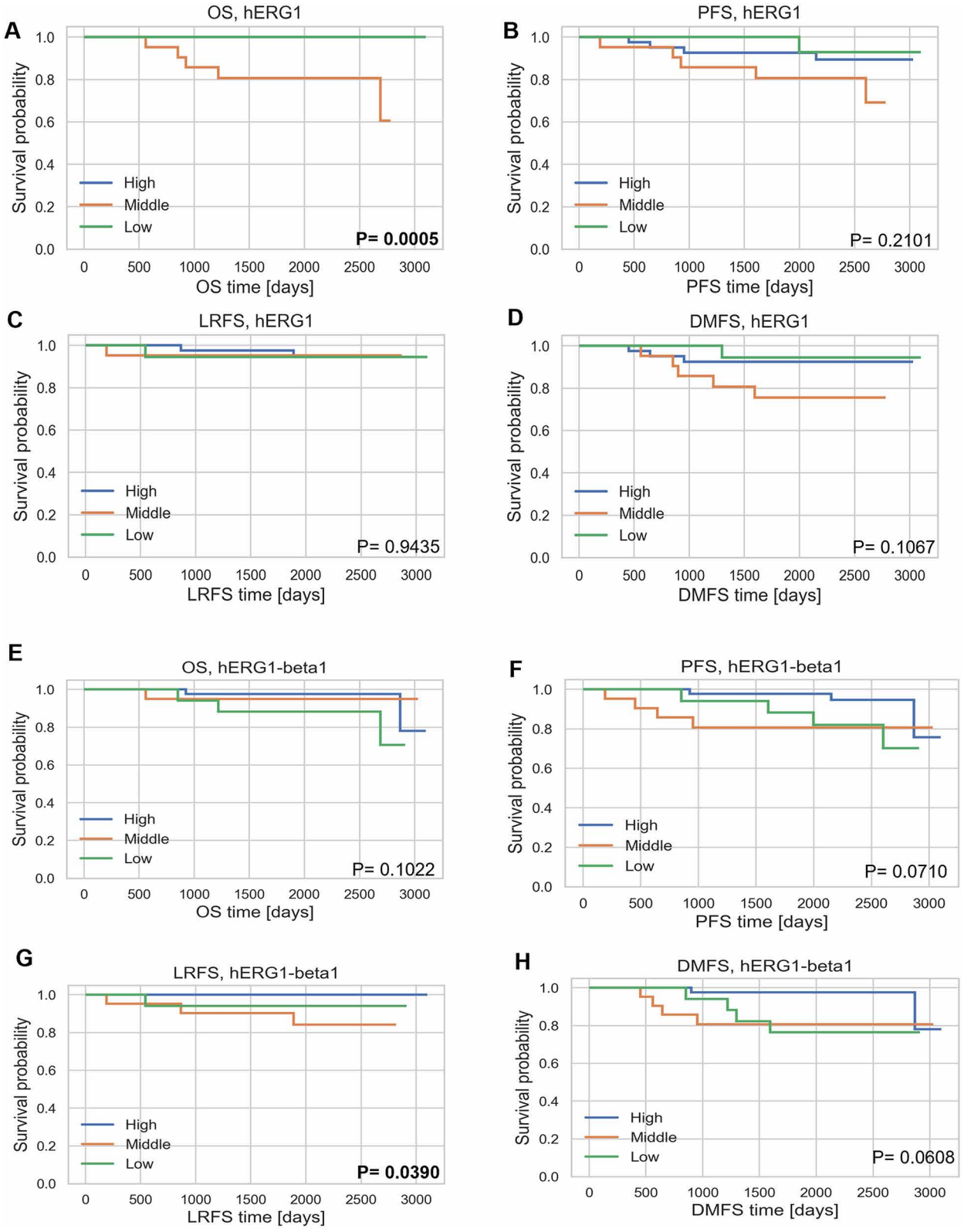

Fig. 7 Survival analyses for hERG1 and hERG1/β1 integrin complex. **A**) Kaplan Meier plots of OS. **B**) Kaplan Meier plots of PFS. **C**) Kaplan Meier plots of LRFS. **D**) Kaplan Meier plots of DMFS. **E**) Kaplan Meier plots of OS. **F**) Kaplan Meier plots of PFS. **G**) Kaplan Meier plots of LRFS. **H**) Kaplan Meier plots of DMFS. *N* = 81

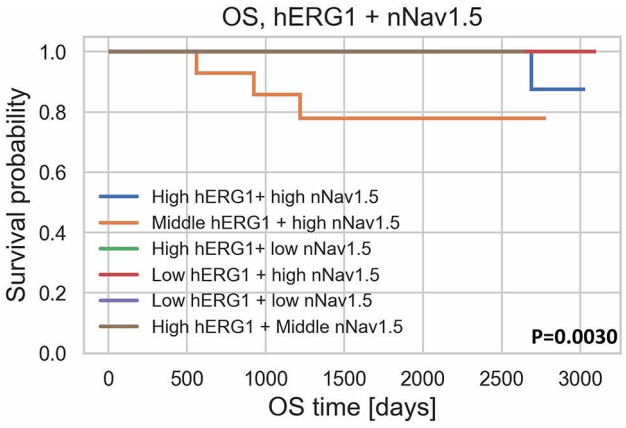

Fig. 8 Combined Kaplan Meier plots of OS according to hERG1 and nNav1.5 levels of expression. *N* = 81

rather than in its individual components, as evidenced by data obtained from BCa cell lines [31] and corroborated by the IHC data presented in this paper.

KCNH2 and *SCN5A* genes correlation

In this paper we showed for the first time that *KCNH2* and *SCN5A* (two of the most relevant ion channels encoding genes in BCa) are co-expressed in BCa and that a correlation exists within a precise range of expression level. The expression of the transcripts appears to be highly correlated in the human heart, as expected since the two channels play a major role in the cardiac tissue. In fact, both hERG1 and Nav1.5 channels are involved in cardiac function and it is well known that mutations of the corresponding genes are frequently associated with arrhythmias and are the main cause of Long QT Syndromes [32]. On the contrary, mutations of these genes in tumors are not frequent, as we showed in this paper through an in silico approach. Interestingly, when we analyzed the distribution of the expression levels, we observed a rather broad distribution in healthy breast tissue and even more (almost twice as broad) in BCa. We also showed, for the first time, that the expression levels are correlated since higher levels of *KCNH2* were associated with higher *SCN5A*. Interestingly, the correlation between the two genes appears in a consistent way only within an intermediate range of expression, suggesting that when the levels are too low or too high, they do not associate and cooperate. Moreover, the two genes were included in a gene network also comprising *ITGB1* (encoding the β1 integrin) and *SLC9A1* (encoding NHE1). The gene network includes other cancer-relevant genes, such as *COL4A5*, *CCN1* and *ADGRF4*, which may cooperate with the aforementioned genes to promote a more invasive phenotype to the cells. Additionally, the network contains genes associated with the cell cycle and proliferation, such as *CCND2*. Moreover, the gene network includes another transporter, *SLC7A5*, which encodes the L-Type Amino Acid Transporter 1. Overall, our data contribute to clarify the complex genetic picture of BCa, highlighting the relevance and networking of ion channels and receptors encoding genes in such disease.

NHE1, hERG1, β1 integrin and nNa$_v$1.5 proteins in BCa

The expression of hERG1 and nNav1.5 channels in BCa was already shown, as separate entities. In particular, hERG1 was shown to be expressed in BCa primary tissues belonging to all the different molecular subtypes and its expression contributes to identify patients with better outcome [7]. In BCa, hERG1 was reported to induce cell senescence [6], besides regulating cell cycle progression [33], and to contribute to triggering metastatic spread in mouse models [16]. This effect was traced back to the occurrence of a hERG1/β1 integrin complex that is exclusively expressed in tumor tissue at difference from healthy tissues [16]. We recently demonstrated that the hERG1/β1 integrin complex is present in various tumor cell lines and follows a specific dynamic pattern [31]. Moreover, β1 integrin stimulation promotes the translocation of the hERG1 channel on the cell membrane thereby enhancing its activation [31]. Specifically, β1 integrin activation increases the amplitude of the IKr by stimulating hERG1 expression and translocation to the plasma membrane without altering its biophysical properties [31]. The slow kinetics of hERG1 cycling are supported by the prolonged lifespan of the hERG1/β1 integrin complex, which preferentially recruits channels in the closed state, thereby slowing down hERG1 degradation. Consistently, channels recruited in the closed state within the complex are less susceptible to degradation mediated by RAB5 [31].

We also demonstrated that the hERG1/β1 integrin complex is expressed in several cell lines and primary tumors [34]. In BCa cell lines we further showed that this complex includes two additional components: nNav1.5 and NHE1 [18].

The expression and functional role of nNa$_V$1.5 in BCa has been extensively characterized by pivotal work from Djamgoz's group [10, 35], and further confirmed independently by other groups [9]. The main role of this sodium channel in BCa is its involvement in the metastatic process, as occurs for several voltage-gated sodium channels in other cancer types [36]. Moreover, the expression of the neonatal form of Na$_V$1.5 was detected in BCa cells [10, 11] and addressed as the main isoform of this channel type.

Once highlighted the relationship between the four genes we moved down this line and analyzed the expression of the corresponding proteins through IHC. Specifically, employing a novel monoclonal antibody developed and characterized by us (Duranti C et al., manuscript in

preparation) we provided further evidence for the that $nNa_V1.5$ is expressed in BCa primary samples, supporting earlier work involving a polyclonal antibody [37]. What is more, we showed here that hERG1 and $nNa_V1.5$ channels are co- expressed in BCa primary samples along with β1 integrin and NHE1. From these analyses it emerged that the expression of the proteins was significantly correlated, with statistically significant P values associated to Pearson's correlation coefficient. Moreover, both channels (as well as the hERG1/β1 integrin complex) were statistically associated with molecular subtype (showing higher expression in Luminal A and Luminal B subtype, respectively) and with hormone receptors (ER and PgR). Additionally, hERG1 (and its complex with β1 integrin) also associated with G2 and HER2 expression. These results are in accordance with our previously published data [7] showing that hERG1 is associated with Luminal A molecular subtype, grading, ER. At difference from our previous published data [7], in the cohort analyzed in the present paper we did not highlight any association with Ki67 proliferative index. In this paper we also highlighted a significant association with HER2 expression strengthening the findings of our previous paper [7]. A few papers have been addressing the expression and role of sodium channel Nav1.5 in BCa, some of them focusing on the adult isoform and some other dealing with the neonatal isoform as our paper. Specifically, a paper by Nelson and colleagues evaluated 66 BCa samples but no associations with either clinical features or survival emerged [38]. A paper by Yamaci and colleagues evaluated the association of nNav1.5 in a small cohort (38 patients) and they highlighted an association with ER expression, although not significant [39]. At difference from our results, no associations with PgR emerged and HER2 was not evaluated. More recently, a preprint by the group of Dr Brackenbury was reported the analysis of a wide cohort of BCa patients ($n = 1740$) [40]. In such study, a different scoring system from the one we applied in the present paper was used and the evaluation was not focused on nNav1.5. The Authors reported significant associations with ER, PgR and HER2 (in accordance with our present data) although the direction of the correlation is unclear since in text and table opposite information is reported. Survival analyses showed that patients with middle expression of hERG1 had lower OS (in accordance with what we obtained analyzing *KCNH2* in TCGA datasets). In this view, it should be pointed out that survival analyses performed with IHC data were carried out in a smaller group of patients when compared with the TCGA datasets that were also characterized by longer follow-up time. This might be the main reason of the discrepancy observed, along with the fact that analyzing RNA (like in RNASeq data stored in TCGA datasets) or proteins (like IHC studies performed on formalin fixed paraffin embedded samples) might provide different results, in any case. Moreover, different cut-off setting methods are used for RNASeq and IHC therefore differences among the groups might also be due to such aspect.

Interestingly, the same result was obtained when considering LRFS according to the hERG1/β1 integrin complex. Again, these data corroborate and strengthen our previous results in which we obtained the same trend (PFS, LRFS and DMFS) for progression-free survival, although significance was not reached [7]. The finding that middle hERG1 expression are associated with poorer survival could be traced back to the fact that part of the channel is complexed with β1 integrin and part is present as a single entity, therefore it could be argued that the complex rather than hERG1 channel alone plays a major role in BCa. Nevertheless, it is important to underline that the analysis of hERG1 alone or complexed with β1 integrin gave overlapping results and that the clinical relevance of the complex was reported here for the first time. The survival analyses according nNav1.5 expression did not highlight any statistically significant difference. These results differ from what reported by Leslie and colleagues that stated that high $Na_V1.5$ expression was associated with a significant reduction in DMFS, OS, LRFS, Disease Free Survival and Cancer Specific Survival although as previously stated they did not focus on the neonatal isoform (moreover, the data are not reported in the main text and the Supplementary are not available as a preprint therefore it is not straightforward to compare their results with ours) [40].

Finally, we showed here for the first time that hERG1 and $nNa_V1.5$ co-expression had an impact on survival. In particular, BCa patients with middle hERG1 and high $nNa_V1.5$ showed significantly compromised overall survival, reflecting presumably metastatic disease, the main cause of death from cancer. Indeed, the combination of the two channels only partially aligns with the metastasis model proposed by Djamgoz [41]. Our data indicate that, at least in the case of hERG1, its biological relevance in cancer cells is more closely associated with its role in activating downstream signaling pathways activators than with its canonical ion-conductive behavior. Specifically, the finding that the hERG1 channel is recruited into the complex in its closed state underscores its importance as a signal-generating protein rather than as an ion channel. In conclusion, our data, taken together, contribute to shed some light in the multifaceted portrait of ion channel involvement in human cancer and we provided here the first demonstration of the co-expression and clinical relevance of hERG1 and nNav1.5 channels in BCa both at gene and protein levels. The immunohistochemistry results presented in this paper corroborate and confirm our previous findings in BCa cells [18], demonstrating that the four proteins involved in forming the

macromolecular complex (NHE1, hERG1, β1 integrin and nNa$_V$1.5) are also present and correlated in primary samples. Moreover, potassium and sodium channels as well as the complex with integrin receptors show clinical relevance thus representing a novel functional biomarker that could assist clinical management of BCa patients. Overall, these findings pave the road for further studies aimed at identifying novel therapeutic targets, mostly needed for TNBC tumors characterized by the worst outcome. Moreover, results obtained in several in vitro models demonstrated the efficacy of hERG1/β1 integrin blockage [35] and the results presented in this paper might serve as a starting point to propose combined therapies targeting the complex (through the bispecific antibody also used in this paper) and sodium channels such as Ranolazine [42, 43], after proper validation in preclinical studies.

Methods

In-silico analysis

An in-silico analysis was carried out using UCSC Xena Browser (University of California, Santa Cruz, http://xena.ucsc.edu/) [44]. This browser allows the direct comparison of gene expression in tumor datasets stored in the TCGA library with healthy samples from the GTEx database (https://gtexportal.org/home/) [45]. The TCGA data were filtered to keep only BCa samples ($n = 1278$) while, for the control group, healthy breast samples retrieved from GTEx ($n = 179$) were used. A Gene Set Enrichment Analysis (GSEA) was carried out with an implemented version of the software (blitzGSEA) [46] to identify the enriched pathway in the BCa cohort under study. A differentially expressed gene (DEGs) analysis was performed with UCSC Xena Browser following the pipeline adapted from Dr Ma'ayan's group (https://appyters.maayanlab.cloud/#/Bulk_RNA_seq). Such pipeline allowed us to analyze both DEGs, Gene Ontology (GO) terms [47] and KEGG (KEGG (RRID: SCR_012773), Kyoto Encyclopedia of Genes and Genomes) pathways [48]. The analysis was performed through the Enrichr web tool [19].

Correlation analysis was carried out with Breast Cancer Gene-Expression Miner v5.0 (bc-GenExMiner v5.0, http://bcgenex.ico.unicancer.fr/BC-GEM/GEM-Requete.php?mode=10) [49].

Moreover, a gene network analysis and a Gene Set Variation Analysis (GSVA) analysis were carried out using Gene Friends (https://genefriends.org/start/input) [23] and Gene Set Cancer Analysis (GSCA, https://guolab.wchscu.cn/GSCA), respectively. Specifically, GSVA estimates the variation in gene set activity (represented as the GSVA score) across the BCa sample population in an unsupervised manner. The GSVA score was calculated using the R package GSVA.

Human samples

A retrospective study was carried out on a set of 81 human BCa samples (representative of the four main pathological subtypes) made available by the archives of the Department of Health Sciences, Division of Pathological Anatomy, University of Florence, after informed written consent and ethical committee approval. Each case was assessed by an experienced breast pathologist. The patients had not received any drug treatment prior to surgery. Molecular subtype was determined by examining ER, PgR and HER2 status for each case. Hormone receptor status was determined by immunostaining as negative when < 1% of tumours cells stained; HER2 status was determined in cases scored as 0 or 1+ (negative) and 3+ (positive). In addition, confirmatory in situ hybridization (FISH) was used in cases scored as 2+.

Clinical data were retrieved from the Archimed database of the Radiation Oncology Unit, Oncology Department, Azienda Ospedaliero Universitaria Careggi, Florence, Italy, where patients were followed up. In particular, the following parameters were considered: molecular subtype, grading, TNM stage, ki67 level of expression, ER, PgR and ER expression, occurrence of local relapse, presence of distant metastases, progression of the disease, overall survival.

Immunohistochemistry (IHC)

IHC was performed on formalin-fixed, paraffin-embedded human archival pathological samples using the following antibodies: anti NHE1 (Polyclonal / anti-NHE1, Novus Biologicals, Centennial, CO, USA, 1:400), anti-hERG1 (mAb-hERG1, MCK Therapeutics Srl, Pistoia, Italy; 1:500 final dilution), anti-hERG1/β1 integrin (scDb, MCK Therapeutics Srl, Pistoia, Italy; 1:50), anti-nNav1.5 (mAb-nNav1.5, Celex Holding Limited, London, UK; 1:200). The procedure was that reported by our group [7, 24, 25] for hERG1, hERG1/β1 integrin and NHE1. For nNa$_V$1.5 the same procedure was followed except for antigen retrieval, carried out by heating the samples in a microwave oven at 600 W in citrate buffer pH 6.0 for 3 min.

Immunostaining was carried out with a commercially available kit (PicTure-Max polymer Detection kit, Invitrogen) according to manufacturer's instructions and to previous papers from our group [7, 24, 25, 50, 51]. Samples were evaluated by three independent investigators (EL, JI and SB), and staining in the tumor area was compared with healthy peri-tumoral tissue, which served as a negative internal control.

Expression was quantified using the following parameters:

1) Intensity (I) - rated as 0 (negative), 1 (weak), 2 (moderate) and 3 (strong).

2) Extent (Ext) - percentage of immunoreactive cells.

A combined IHC score (IS) was obtained as "I x Ext" and the values of IS were grouped for statistical convenience as final "immunohistochemical scores" (IHCSs) as follows: IHCS = 0 (TS = 0), IHCS = 1 (TS = 1-100), IHCS = 2 (TS = 101–200) and IHCS = 3 (TS = 201–300). This method is frequently applied in similar conditions when working with cytoplasmic/membrane proteins [52].

Statistical analysis

The presence of association between demographic, clinical and biological characteristics as well as the association between biomarkers' expression was evaluated by Fisher's exact test (two-tailed, $p < 0.05$). The Shapiro-Wilk test was applied to evaluate normality. Because the data did not follow a normal distribution, a non-parametric test was applied in the analysis. The Spearman correlation coefficient (rho) was calculated to evaluate relationships between continuous variables (rho = – 1 negative relationship; rho = 0 no relationship; rho = 1 positive relationship). Survival analyses were carried out by performing Log Rank Test and Kaplan-Meier analyses. Overall Survival (OS) was calculated from the date of diagnosis to the date of death or the date of last follow-up. Progression Free Survival (PFS), Local Relapse Free Survival (LRFS) and Distant Metastases Free Survival (DMFS) were calculated as the time between the date of diagnosis and the first date of progression/relapse/metastasis development or death, whichever comes first, or last tumor evaluation.

Statistical analyses were performed using Stata 9.1 (Stata (RRID: SCR_012763), StataCorp, TX, USA), GraphPad Prism version 10 (GraphPad Prism (RRID: SCR_002798), GraphPad Software, MA, USA) and custom-coded Phyton scripts for Kaplan Meier plots.

Supplementary Information

The online version contains supplementary material available at https://doi.org/10.1186/s12935-025-03653-w.

Supplementary Material 1

Author contributions

AA and EL conceived the study. IM and SB recruited the patients and collected samples and relevant clinical information. IM collected relevant clinical information. EL, JI, FP, CC, MS, SPF and CD performed the experiments and analyses. EL, JI, FP, CC, MBAD, AB and AA interpreted the data. EL, FP and JI drafted the manuscript and prepared figures and tables. All authors read and approved the final manuscript.

Funding

This research was funded by the University of Florence to AA and EL, by Associazione Italiana per la Ricerca sul Cancro (grant 1662, 15627 and 21510) to AA; grants by the European Union - NextGenerationEU - National Recovery and Resilience Plan, Mission 4 Component 2 - Investment 1.5 - THE - Tuscany Health Ecosystem - ECS00000017 - CUP B83C22003920001 to AA; grants by European Union, National Recovery and Resilience Plan, Mission 4 Component 2 – Investment 1.4 - National Center for Gene Therapy and Drugs based on RNA Technology - NextGenerationEU – Project Code CN00000041-CUP B13C22001010001 to AA. JI was supported by Regione Toscana fellowship within the project "Progetti di alta formazione attraverso l'attivazione di Assegni di Ricerca" (MutCoP project) co-funded by Fondazione Cassa di Risparmio di Pistoia e Pescia and was formerly funded by a fellowship of Fondazione Cassa di Risparmio di Pistoia e Pescia within Giovani@Ricerca Scientifica program.

Data availability

The datasets used and/or analyzed during the present study are available from the corresponding author on reasonable request.

Declarations

Ethics approval and consent to participate

All the patients were enrolled after informed written consent. The study was approved by the local Ethical Committee of Azienda Ospedaliero-Universitaria Careggi (BIO.16.028).

Consent for publication

Not applicable.

Competing interests

The authors declare no competing interests.

Author details

[1]Department of Experimental and Clinical Medicine, University of Florence, Florence, Italy
[2]CSDC (Center for the Study of complex dynamics), University of Florence, Florence, Italy
[3]Department of Physics, University of Florence and Florence Section of INFN, Florence, Italy
[4]Department of Medical Biotechnologies, University of Siena, Siena, Italy
[5]MCK Therapeutics Srl, Pistoia, Italy
[6]Department of Health Sciences, Division of Pathological Anatomy, University of Florence, Florence, Italy
[7]Department of Experimental and Clinical Biomedical Sciences Mario Serio, University of Florence, Florence, Italy
[8]Radiation Oncology Unit, Oncology Department, Azienda Ospedaliero Universitaria Careggi, Florence, Italy
[9]Department of Life Sciences, Imperial College London, London, UK
[10]Biotechnology Research Centre, Cyprus International University, Mersin 10, Haspolat, TRNC, Turkey
[11]Department of Biotechnology and Biosciences, University of Milano Bicocca, Milan, Italy

Received: 10 August 2024 / Accepted: 15 January 2025
Published online: 26 January 2025

References

1. Sung H, Ferlay J, Siegel RL, Laversanne M, Soerjomataram I, Jemal A, et al. Global Cancer statistics 2020: GLOBOCAN estimates of incidence and Mortality Worldwide for 36 cancers in 185 countries. CA Cancer J Clin. 2021;71:209–49.
2. Perou CM, Sørile T, Eisen MB, Van De Rijn M, Jeffrey SS, Ress CA, et al. Molecular portraits of human breast tumours. Nat 2000. 2000;406:6797.
3. Lee A, Djamgoz MBA. Triple negative breast cancer: emerging therapeutic modalities and novel combination therapies. Cancer Treat Rev. 2018;62:110–22.
4. Prevarskaya N, Skryma R, Shuba Y. Ion channels in Cancer: are Cancer Hallmarks oncochannelopathies? Physiol Rev. 2018;98:559–621.
5. Lastraioli E, Iorio J, Arcangeli A. Ion channel expression as promising cancer biomarker. Biochim et Biophys Acta (BBA) - Biomembr. 2015;1848:2685–702.
6. Lansu K, Gentile S. Potassium channel activation inhibits proliferation of breast cancer cells by activating a senescence program. Cell Death & Disease. 2013;4:e652–e652.

7. Iorio J, Meattini I, Bianchi S, Bernini M, Maragna V, Dominici L et al. hERG1 channel expression associates with molecular subtypes and prognosis in breast cancer. Cancer Cell Int. 2018;18.
8. Djamgoz MBA, Fraser SP, Brackenbury WJ. In Vivo evidence for Voltage-gated Sodium Channel Expression in Carcinomas and Potentiation of Metastasis. Cancers (Basel). 2019;11.
9. Roger S, Besson P, Le Guennec JY. Involvement of a novel fast inward sodium current in the invasion capacity of a breast cancer cell line. Biochim Biophys Acta Biomembr. 2003;1616:107–11.
10. Fraser SP, Diss JKJ, Chioni AM, Mycielska ME, Pan H, Yamaci RF, et al. Voltage-gated sodium channel expression and potentiation of human breast cancer metastasis. Clin Cancer Res. 2005;11:5381–9.
11. Brackenbury WJ, Chioni AM, Diss JKJ, Djamgoz MBA. The neonatal splice variant of Nav1.5 potentiates in vitro invasive behaviour of MDA-MB-231 human breast cancer cells. Breast Cancer Res Treat. 2007;101:149–60.
12. Nelson M, Yang M, Dowle AA, Thomas JR, Brackenbury WJ. The sodium channel-blocking antiepileptic drug phenytoin inhibits breast tumour growth and metastasis. Mol Cancer. 2015;14.
13. Luo Q, Wu T, Wu W, Chen G, Luo X, Jiang L et al. The functional role of Voltage-gated Sodium Channel Nav1.5 in metastatic breast Cancer. Front Pharmacol. 2020;11.
14. Onkal R, Mattis JH, Fraser SP, Diss JKJ, Shao D, Okuse K, et al. Alternative splicing of Nav1.5: an electrophysiological comparison of 'neonatal' and 'adult' isoforms and critical involvement of a lysine residue. J Cell Physiol. 2008;216:716–26.
15. Potier-Cartereau M, Raoul W, Weber G, Mahéo K, Rapetti-Mauss R, Gueguinou M, et al. Potassium and Calcium Channel Complexes as novel targets for Cancer Research. Rev Physiol Biochem Pharmacol. 2022;183:157–76.
16. Becchetti A, Crescioli S, Zanieri F, Petroni G, Mercatelli R, Coppola S et al. The conformational state of hERG1 channels determines integrin association, downstream signaling, and cancer progression. Sci Signal. 2017;10.
17. Hodgkin AL, Huxley AF. A quantitative description of membrane current and its application to conduction and excitation in nerve. 1952. Bull Math Biol. 1990;52:25–71.
18. Capitani C, Iorio J, Lastraioli E, Duranti C, Bagni G, Altadonna GC et al. An integrin centered complex coordinates ion transport and pH to regulate f-actin organization and cell migration in breast cancer. bioRxiv [Internet]. 2024 [cited 2024 Nov 10]; Available from: https://doi.org/10.1101/2024.07.02.601509
19. Kuleshov MV, Jones MR, Rouillard AD, Fernandez NF, Duan Q, Wang Z et al. Enrichr: a comprehensive gene set enrichment analysis web server 2016 update. Nucleic Acids Res [Internet]. 2016 [cited 2024 Nov 10];44:W90–7. Available from: https://pubmed.ncbi.nlm.nih.gov/27141961/
20. Liberzon A, Birger C, Thorvaldsdóttir H, Ghandi M, Mesirov JP, Tamayo P. The Molecular signatures database (MSigDB) hallmark gene set collection HHS Public Access. Cell Syst. 2015;1:417–25.
21. Sanguinetti MC, Jiang C, Curran ME, Keating MT. A mechanistic link between an inherited and an acquired cardiac arrhythmia: HERG encodes the IKr potassium channel. Cell [Internet]. 1995 [cited 2025 Jan 4];81:299–307. Available from: https://pubmed.ncbi.nlm.nih.gov/7736582/
22. Abriel H. Roles and regulation of the cardiac sodium channel Na v 1.5: recent insights from experimental studies. Cardiovasc Res [Internet]. 2007 [cited 2025 Jan 4];76:381–9. Available from: https://pubmed.ncbi.nlm.nih.gov/17727828/
23. Raina P, Guinea R, Chatsirisupachai K, Lopes I, Farooq Z, Guinea C et al. GeneFriends: gene co-expression databases and tools for humans and model organisms. Nucleic Acids Res [Internet]. 2023 [cited 2024 Nov 10];51:D145–58. Available from: https://pubmed.ncbi.nlm.nih.gov/36454018/
24. Duranti C, Iorio J, Lottini T, Lastraioli E, Crescioli S, Bagni G et al. Harnessing the hERG1/β1 Integrin Complex via a Novel Bispecific Single-chain Antibody: An Effective Strategy against Solid Cancers. Mol Cancer Ther. 2021;20:molcanther.1111.2020.
25. Lottini T, Duranti C, Iorio J, Martinelli M, Colasurdo R, D'Alessandro FN et al. Combination therapy with a bispecific antibody targeting the hERG1/β1 Integrin Complex and gemcitabine in pancreatic ductal adenocarcinoma. Cancers (Basel). 2023;15.
26. Fukushiro-Lopes DF, Hegel AD, Rao V, Wyatt D, Baker A, Breuer EK et al. Preclinical study of a Kv11.1 potassium channel activator as antineoplastic approach for breast cancer. Oncotarget [Internet]. 2017 [cited 2023 Feb 2];9:3321–37. Available from: https://pubmed.ncbi.nlm.nih.gov/29423049/
27. Klahan S, Huang WC, Chang CM, Wong HSC, Huang CC, Wu MS, et al. Gene expression profiling combined with functional analysis identify integrin beta1 (ITGB1) as a potential prognosis biomarker in triple negative breast cancer. Pharmacol Res. 2016;104:31–7.
28. Sun Q, Zhou C, Ma R, Guo Q, Huang H, Hao J et al. Prognostic value of increased integrin-beta 1 expression in solid cancers: a meta-analysis. Onco Targets Ther [Internet]. 2018 [cited 2024 May 30];11:1787–99. Available from: https://pubmed.ncbi.nlm.nih.gov/29636624/
29. Amith SR, Fliegel L. Na+/H + exchanger-mediated hydrogen ion extrusion as a carcinogenic signal in triple-negative breast cancer etiopathogenesis and prospects for its inhibition in therapeutics. Semin Cancer Biol. 2017;43:35–41.
30. Yang M, Kozminski DJ, Wold LA, Modak R, Calhoun JD, Isom LL et al. Therapeutic potential for phenytoin: targeting Na(v)1.5 sodium channels to reduce migration and invasion in metastatic breast cancer. Breast Cancer Res Treat [Internet]. 2012 [cited 2023 Mar 7];134:603–15. Available from: https://pubmed.ncbi.nlm.nih.gov/22678159/
31. Duranti C, Iorio J, Bagni G, Altadonna GC, Fillion T, Lulli M et al. Integrins regulate hERG1 dynamics by girdin-dependent Gαi3: signaling and modeling in cancer cells. Life Sci Alliance [Internet]. 2023 [cited 2024 Nov 11];7. Available from: https://pubmed.ncbi.nlm.nih.gov/37923359/
32. Duranti C, Iorio J, Lottini T, Lastraioli E, Crescioli S, Bagni G et al. Harnessing the hERG1/β1 Integrin Complex via a Novel Bispecific Single-chain Antibody: An Effective Strategy against Solid Cancers. Mol Cancer Ther [Internet]. 2021 [cited 2021 Aug 5];20:molcanther.1111.2020. Available from: https://pubmed.ncbi.nlm.nih.gov/34045227/
33. Perez-Neut M, Rao VR, Gentile S. hERG1/Kv11.1 activation stimulates transcription of p21waf/cip in breast cancer cells via a calcineurin-dependent mechanism. Oncotarget. 2016;7:58893–902.
34. Duranti C, Iorio J, Lottini T, Lastraioli E, Crescioli S, Bagni G et al. Harnessing the hERG1/β1 Integrin Complex via a Novel Bispecific Single-chain Antibody: An Effective Strategy against Solid Cancers. Mol Cancer Ther [Internet]. 2021 [cited 2024 Nov 11];20:1338–50. Available from: https://pubmed.ncbi.nlm.nih.gov/34045227/
35. Fraser SP, Salvador V, Manning EA, Mizal J, Altun S, Raza M, et al. Contribution of functional voltage-gated na + channel expression to cell behaviors involved in the metastatic cascade in rat prostate cancer: I. lateral motility. J Cell Physiol. 2003;195:479–87.
36. Onkal R, Djamgoz MBA. Molecular pharmacology of voltage-gated sodium channel expression in metastatic disease: clinical potential of neonatal Nav1.5 in breast cancer. Eur J Pharmacol. 2009;625:206–19.
37. Fraser SP, Diss JKJ, Chioni AM, Mycielska ME, Pan H, Yamaci RF et al. Voltage-gated sodium channel expression and potentiation of human breast cancer metastasis. Clin Cancer Res [Internet]. 2005 [cited 2024 May 6];11:5381–9. Available from: https://pubmed.ncbi.nlm.nih.gov/16061851/
38. Nelson M, Yang M, Millican-Slater R, Brackenbury WJ. Nav1.5 regulates breast tumor growth and metastatic dissemination in vivo. Oncotarget [Internet]. 2015 [cited 2021 Jun 15];6:32914–29. Available from: https://pubmed.ncbi.nlm.nih.gov/26452220/
39. Yamaci RF, Fraser SP, Battaloglu E, Kaya H, Erguler K, Foster CS et al. Neonatal Nav1.5 protein expression in normal adult human tissues and breast cancer. Pathol Res Pract [Internet]. 2017 [cited 2021 Jun 15];213:900–7. Available from: https://pubmed.ncbi.nlm.nih.gov/28698102/
40. Leslie TK, Tripp A, James AD, Fraser SP, Nelson M, Sajjaboontawee N et al. A novel Nav1.5-dependent feedback mechanism driving glycolytic acidification in breast cancer metastasis. Oncogene [Internet]. 2024 [cited 2025 Jan 4];43:2578–94. Available from: https://pubmed.ncbi.nlm.nih.gov/39048659/
41. Djamgoz MBA. Electrical excitability of cancer cells-CELEX model updated. Cancer Metastasis Rev [Internet]. 2024 [cited 2024 Aug 10]; Available from: https://pubmed.ncbi.nlm.nih.gov/38976181/
42. Driffort V, Gillet L, Bon E, Marionneau-Lambot S, Oullier T, Joulin V et al. Ranolazine inhibits NaV1.5-mediated breast cancer cell invasiveness and lung colonization. Mol Cancer [Internet]. 2014 [cited 2023 Apr 26];13. Available from: https://pubmed.ncbi.nlm.nih.gov/25496128/
43. Djamgoz MBA. Ranolazine: a potential anti-metastatic drug targeting voltage-gated sodium channels. British Journal of Cancer 2024 130:9 [Internet]. 2024 [cited 2024 Jun 6];130:1415–9. Available from: https://www.nature.com/articles/s41416-024-02622-w
44. Goldman MJ, Craft B, Hastie M, Repečka K, McDade F, Kamath A, et al. Visualizing and interpreting cancer genomics data via the Xena platform. Nat Biotechnol 2020. 2020;38:6.
45. Consortium TGte. The GTEx Consortium atlas of genetic regulatory effects across human tissues. Sci (1979). 2020;369:1318–30.
46. Lachmann A, Xie Z, Ma'ayan A. blitzGSEA: efficient computation of gene set enrichment analysis through gamma distribution approximation.

Bioinformatics [Internet]. 2022 [cited 2024 May 6];38:2356–7. Available from: https://pubmed.ncbi.nlm.nih.gov/35143610/
47. Ashburner M, Ball CA, Blake JA, Botstein D, Butler H, Cherry JM et al. Gene Ontology: tool for the unification of biology The Gene Ontology Consortium* [Internet]. 2000. Available from: http://www.flybase.bio.indiana.edu
48. Kanehisa M, Goto S. KEGG: Kyoto Encyclopedia of Genes and Genomes. Nucleic Acids Res [Internet]. 2000 [cited 2024 Mar 16];28:27–30. Available from: http://www.genome.ad.jp/kegg/
49. Jézéquel P, Frénel JS, Campion L, Guérin-Charbonnel C, Gouraud W, Ricolleau G et al. bc-GenExMiner 3.0: New mining module computes breast cancer gene expression correlation analyses. Database. 2013;2013.
50. Muratori L, Petroni G, Antonuzzo L, Boni L, Iorio J, Lastraioli E et al. HERG1 positivity and Glut-1 negativity identifies high-risk TNM stage I and II colorectal cancer patients, regardless of adjuvant chemotherapy. Onco Targets Ther. 2016;9.
51. Lastraioli E, Fraser S, Guzel R, Iorio J, Bencini L, Scarpi E, et al. Neonatal Nav1.5 protein expression in human colorectal Cancer: immunohistochemical characterization and clinical evaluation. Cancers (Basel). 2021;13:3832.
52. Perrone G, Santini D, Vincenzi B, Zagami M, La Cesa A, Bianchi A et al. COX-2 expression in DCIS: correlation with VEGF, HER-2/neu, prognostic molecular markers and clinicopathological features. Histopathology [Internet]. 2005 [cited 2024 May 10];46:561–8. Available from: https://pubmed.ncbi.nlm.nih.gov/15842638/

Publisher's note